

Neutron Spectra from the 38.8-MeV Alpha-Particle Bombardment of Deuterium*

C. W. Lewis, D. P. Saylor,† and L. C. Northcliffe

Cyclotron Institute, Texas A & M University, College Station, Texas 77843

(Received 10 July 1970)

The energy spectra of neutrons from the α -particle bombardment of deuterium at 38.8 MeV have been measured at lab angles of 15, 18, 21, 24, 30, 45, and 54°. Prominent features of the spectra are explainable on simple kinematic bases. The shapes of the energy spectra and the cross-section values are consistent with the calculations of Shanley and Nakamura but seem to be inconsistent with proton spectra from the same reaction as measured by Nagatani, Tombrello, and Bromley.

I. INTRODUCTION

The reaction $\alpha + d \rightarrow n + p + \alpha$ has been the subject of numerous investigations,¹⁻¹³ most of which have been concerned with the detection of the emitted charged particles. The interest in this reaction stems from two features: (1) Below the α -particle breakup energy (19.8 MeV) only one inelastic channel is open, and an especially simple case of a three-body final state can be studied; and (2) measurements of the energy spectra of the emitted particles, in both coincident^{12,13} and noncoincident¹⁻¹¹ modes of detection, show evidence of strong interactions between a nucleon and the α particle in the final state. This second feature has caused us to speculate that the reaction might be used as a source of highly polarized neutrons, since it is well known that high polarization is produced in free nucleon- α scattering. As a preliminary to studies of the polarization of neutrons from this reaction we have measured noncoincident neutron energy spectra by a modified time-of-flight technique.¹⁴ The spectra were measured at laboratory angles between 15 and 54° for α -particle bombarding energy near 40 MeV. The angles and bombarding energy were chosen to facilitate comparison with measurements of the noncoincident proton energy spectra from the same reaction by Nagatani, Tombrello, and Bromley.¹⁰ The only previous measurement of neutron emission at comparable bombarding energy is the 0° measurement by Rybakov, Sidorov, and Vlasov⁶ at 34.6 MeV; all other neutron data^{2,3,7} are for substantially lower energies.

II. EXPERIMENTAL

A. Beam Preparation and Handling

The 40-MeV α -particle beam from the Texas A & M variable energy cyclotron was focused and analyzed by a quadrupole doublet lens and a switching magnet and then brought to a focus on a target in a shielded experimental cave with another quadrupole doublet lens. The transmitted beam,

broadened by multiple scattering in the target, was refocused by a third quadrupole doublet lens and buried in a heavily shielded beam stop approximately 5 m downstream. The shielding of the beam stop consisted of about 1 m³ of steel in the form of horizontally stacked plates around the end of the beam pipe buried in a pile of concrete blocks stacked to an average thickness of about 1 m around the steel core. This refocusing and burial of the transmitted beam greatly reduced the neutron background in the experimental area. The spatial relationships of the beam line components are shown in Fig. 1.

The use of time-of-flight techniques to measure energies of fast neutrons usually presumes a pulsed beam. For flight paths of several meters and neutron energies of 10 MeV or more the time width of each beam pulse should be no greater than 2 or 3 nsec if reasonable energy resolution is to be achieved. For 40-MeV α particles the Texas A & M cyclotron delivers beam pulses separated by 141 nsec with a natural width of 10–15 nsec. It is possible, however, to reduce the width to about 2 nsec full width at half maximum (FWHM) by slightly detuning the cyclotron, that is, by using settings for trim coils, valley coils, ion source position, etc., which differ from those which yield the most intense beam. Usually this sharpening of the time structure of the beam is achieved more easily when a pair of slits in the beam transport system permits transmission of only a well-defined portion of the cyclotron beam. Operation in an off-resonance condition apparently has the effect of reducing the phase interval of the radio frequency dee voltage which is actually effective in the acceleration of beam particles to full energy. The detuning procedure was largely empirical since a set of machine parameters found to produce a narrow time width in one cyclotron run was not necessarily found to do so in the next. Within a given run, however, the time characteristics of a detuned beam showed reasonable long-term stability; experimental runs up to 24 h in length have been

conducted without significant change in the time characteristics.

This technique for reducing the time width of beam pulses is a crude but adequate temporary substitute for the more elegant approach of installing slits in the center region of the cyclotron.¹⁵ Although the detuning caused a reduction of external beam current by a factor of 20–200, the beam current available on target was always more than the 25-nA limit dictated by the necessity to avoid target deterioration.

B. Deuterium Target

Most of the data were obtained with a deuterated polyethylene target, 0.005-in. thickness, in which the energy loss for 40-MeV α particles was 2.3 MeV. Thus the mean bombarding energy was 38.8 MeV. The foil was simply mounted within the beam pipe (3.75-in. o.d., 0.188-in. wall, aluminum) so that the reaction neutrons emerged through a thickness of aluminum which varied with their angle of emission. Correction for the resulting exponential attenuation was made in the usual way using known aluminum total cross sections.¹⁶ Air attenuation was negligible.

Corrections for neutrons from the carbon in the target were obtained at all angles by measuring the neutron spectra from an ordinary polyethylene target of 0.005-in. thickness. The carbon reactions were found to contribute only about 5% of the neutrons observed with CD_2 .

For some of the measurements at small angles and low neutron energies the target was a gas cell 1 in. in length containing four atmospheres of deuterium gas at room temperature. The cell was mounted in a special thin-walled reaction chamber so that neutrons traversed only $\frac{1}{8}$ in. of aluminum in reaching the detector. The entrance and exit windows of the gas cell were Havar foils of 0.000 25-in. thickness. The neutron contribution from the windows was determined by runs with an empty cell.

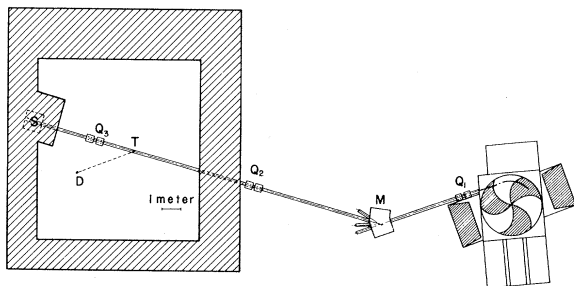


FIG. 1. Experimental layout showing beam preparation and disposal. Q_1 , Q_2 , and Q_3 are quadrupole doublets; M is a deflecting and analyzing magnet; T is the target; D is the detector; S is the shielded beam stop.

C. Neutron Detection System and Method

The time-of-flight versus pulse-height technique used in this experiment has been described in detail elsewhere,¹⁴ so that only a sketch of the method will be given here. Figure 2(a) shows a simplified diagram of the detection system. The neutron detector was a 2-in. diam \times 1-in. cylinder of plastic scintillator (NE102) coupled to an RCA 8575-photomultiplier tube. For each neutron detection event, timing and linear signals taken from the anode and ninth dynode, respectively, were used to generate a time-of-arrival pulse T , of the neutron at the scintillator and a pulse height H from the proton recoil. The timing was relative to a marker generated by the cyclotron rf voltage. Figure 2(b) shows an idealized sketch of the two-parameter T - H distribution to be expected from an accumulation of such events. Figure 3 shows an actual T - H distribution taken with the detector 3 m from the target and at 15° from the beam axis. A background correction, described below, has been subtracted from the spectrum. The average beam pulse width for this spectrum was about 3 nsec, as measured by the width of the γ -ray line. This spectrum and similar ones were taken with a 64×64 two-parameter pulse-height analyzer (Victoreen; SCIPP 4096TP).

D. Monitoring

The relative normalization of each T - H spectrum was provided by a monitor scintillation counter left at a fixed position relative to the target. The time spectrum of monitor pulses, containing a narrow γ -ray peak (mainly from the carbon component of the target) and a broad peak from polyenergetic neutrons (largely from the deuterium of

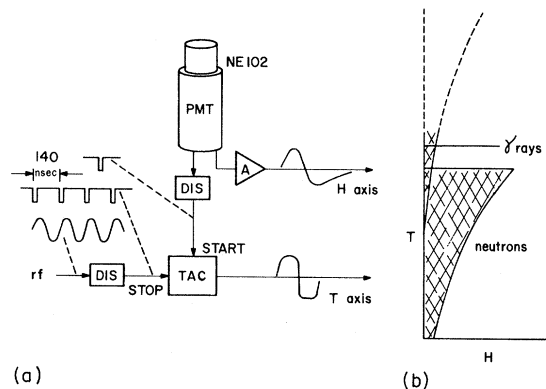


FIG. 2. (a) Schematic diagram of the detection system. (b) Idealized sketch of the two-parameter distribution expected from a continuous distribution of neutron energies.

the target), was accumulated in a second pulse-height analyzer. The proportionality between the total count in the γ -ray peak and the total count in the neutron peak did not change appreciably with time, indicating that target deterioration was not occurring. Thus, the integrated count in either peak could be taken as a relative measure of the number of α particles incident on the target, and used to normalize all T - H distributions relative to one another.

E. Background Elimination

Events in a T - H spectrum which lie outside the "valid" region [the cross-hatched portion of Fig. 2(b)] correspond to background, and can be eliminated by visual inspection. The remaining background was eliminated by the well-known method of inserting a "shadow shield" (a steel cylinder of 6.3-cm diameter and 34-cm length) between target and detector. The resulting background spectrum, properly normalized, was then subtracted from the corresponding T - H spectrum without shadow shield. In any case background was not a severe problem, as it represented only about 10% of the counts in a T - H spectrum.

F. Consistency Checks

For half of the angles investigated measurements were made both to the left and to the right of the beam axis. The difference between left and right measurements at the same angle after normalization and background subtraction as described above was statistically insignificant. This is evidence for the reliability of the relative normalization, the background subtraction, and the experimental alignment. The relative shapes of neutron energy spectra (from the analysis of T - H distribution data) obtained with the deuterium gas target and the deuterated polyethylene foil target agreed wherever such spectra overlapped. The relative shapes of neutron spectra at two angles (21 and 36°) which

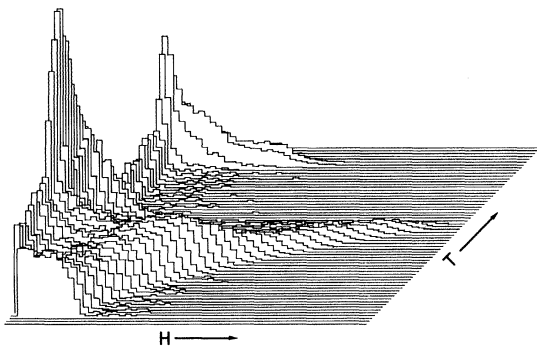


FIG. 3. T - H distribution from 40-MeV α -particle bombardment of CD_2 at $\theta_L = 15^\circ$.

were remeasured in an independent experiment (in which the time width of the cyclotron beam was different from the first measurements) agreed to within a few percent.

III. DATA REDUCTION

A. Analysis of the T - H Distributions

The details of the procedure by which the T - H distributions were converted to neutron energy spectra have been given in Ref. 14. Briefly, the process consists of fitting the distribution of pulse heights H associated with each time channel T with a theoretical pulse-height distribution by the method of linear least squares. Each theoretical pulse-height distribution is calculated from the recoil proton energy distribution, and the response function (maximum pulse height versus neutron energy) and resolution of the scintillator. The expression for the proton energy distribution is taken from the work of Lewis and Blair,¹⁷ and accounts for the distortion produced by those recoil protons which pass out the end of the scintillator before depositing all of their energy. The response and resolution functions are constructed directly from the T - H data. Since the theoretical distribution includes only the effects of the n - p interaction in the scintillator, the portion of the T - H distributions which could include contributions from n -carbon interactions are not considered in the least-square fitting. Evidence is given in Ref. 14 that a theoretical pulse-height distribution constructed as indicated above does adequately represent the data in the appropriate region of the T - H distribution.

The determination of neutron energy is based on time of flight, that is, a conversion of the T axis to neutron energy. This conversion is accomplished in the usual way by first converting the T axis to time of flight, using the centroid of the prompt γ -ray line, and then transforming to neutron energy. The conversion also depends on a calibration of the T axis in terms of nsec/channel, which was determined to about 2% using commercial delay boxes.

B. Absolute Cross-Section Determination

In the calculation of absolute cross sections the most uncertain factors were the number of α particles incident during a run and the number of deuterium nuclei/cm² in the target. The first factor was estimated by measuring the beam current on a removable Faraday cup *upstream* from the target before and after a run, and using the time duration of the run. Over a number of runs the ratio of this estimate to the monitor count remained constant

within a standard deviation of 2%. The absolute accuracy of the Faraday cup calibration was 10%. Unfortunately, the beam current measuring circuitry was changed before a more accurate calibration could be made. The number of deuterium nuclei/cm² in the polyethylene target was determined from the foil thickness and the density of polyethylene (scaled by the factor 16/14) assuming the carbon and deuterium atoms to be in the ratio 1:2. The gas cell density of D₂ was calculated from the pressure and dimensions of the cell. The calculated absolute cross sections of those neutron energy spectra for which both targets were used differed on the average by 6%. The over-all uncertainty in the beam current target density product is estimated to be 15%.

The neutron detection efficiency which enters into the absolute cross-section calculation is implicitly part of the theoretical pulse-height distribution discussed in Sec. III A. Since only that portion of the T - H distribution related to the n - p interaction is fitted, and the much more complicated part which arises from n -carbon interactions is ignored, the efficiency calculation is particularly reliable.

Combining the previous 15% uncertainty with uncertainties from all other sources, the total absolute uncertainty in our measurements is estimated to be no more than 20%.

IV. RESULTS AND DISCUSSION

The measured neutron energy spectra are shown in Figs. 4 and 5. The 45 and 54° measurements were made with a 2-m flight path, the remainder were done at 3 m. The solid curves in the same figures represent the *proton* energy spectra measurements of Nagatani, Tombrello, and Bromley¹⁰ from the same reaction at an α -bombardment energy of 41.6 MeV. An obvious feature of the proton spectra is the prominent peak at the high-energy end of each spectrum whose energy has been shown to agree with that expected from the two-body reaction $\alpha + d \rightarrow p + {}^5\text{He}(\text{g.s.})$, $Q = -3.18$ MeV. In Figs. 4 and 5 the arrows indicate the expected neutron energies from the analogous reaction $\alpha + d \rightarrow n + {}^5\text{Li}(\text{g.s.})$, $Q = -4.19$ MeV. It is apparent that the positions do approximately coincide with the onset of an abrupt decrease in the cross section at each angle, which might be interpreted as a peak smeared by the effect of the target thickness and the finite time width of each beam pulse. In Table I these two effects are assessed for each angle and added in quadrature to obtain the total energy spread expected. With these spreads, a peak of about the same relative size as observed in the proton spectra would take on the appearance seen here. In any event it should be noted that the maximum neutron energy observed at each angle

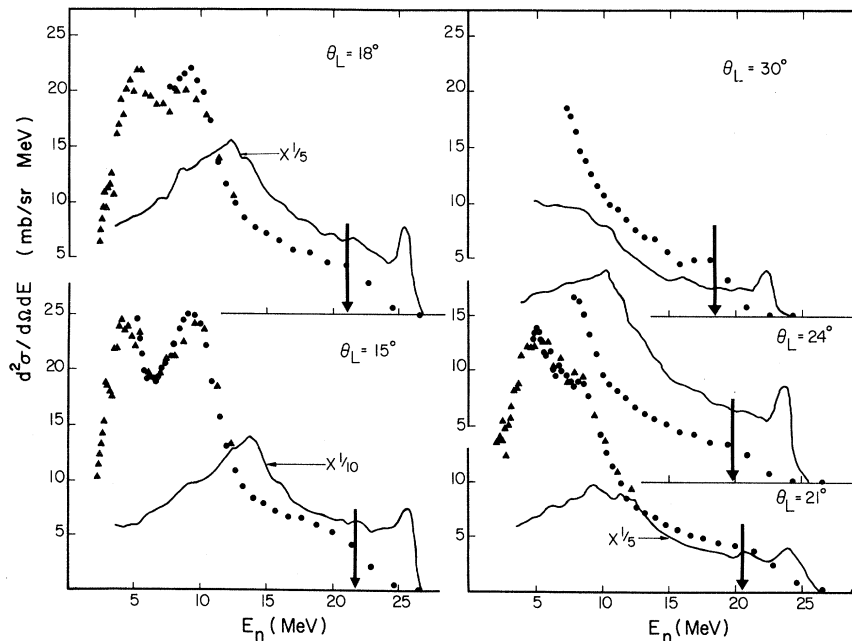


FIG. 4. Laboratory differential cross sections for neutron and proton emission at various laboratory angles, from $\alpha + d$. The abscissa represents laboratory neutron or proton energy. The circles represent neutron data obtained with a deuterated polyethylene target. The triangles represent neutron data obtained with a deuterium gas target. The solid curves represent proton data taken from Ref. 10, measured at 41.6-MeV α -particle bombarding energy. The arrows indicate the expected neutron energy for the process $\alpha + d \rightarrow n + {}^5\text{Li}(\text{g.s.})$.

TABLE I. Contributions to total neutron energy spread at each angle of observation.

Angle	Neutron energy E_n for ${}^5\text{Li(g.s.)}$ (MeV)	Beam width (FWHM) (nsec)	ΔE_n at energy E_n		Total (FWHM) (MeV)
			From beam width (MeV)	From target energy loss (MeV)	
15	21.6	2.5	2.1	2.0	2.9
18	21.1	1.3	1.1	2.0	2.3
21	20.5	2.5	2.1	2.0	2.9
24	19.8	1.3	1.1	1.9	2.2
30	18.3	1.3	0.9	1.8	2.0
36	16.6	2.5	1.5	1.6	2.2
45	13.9	1.3	0.9	1.4	1.7
54	11.0	2.5	1.2	1.2	1.7

agrees quite well with that calculated from the effective two-body reaction $\alpha + d \rightarrow n + (p + {}^4\text{He})$, $Q = -2.23$ MeV, which defines the kinematic absolute maximum for neutron production.

A second feature of the neutron spectra which is worthy of comment is the double peak whose valley occurs around 7 MeV observable in the 15 and 18° spectra, and to a lesser extent at 21°. This feature is due to the sequential reaction $\alpha + d \rightarrow p + {}^5\text{He(g.s.)} \rightarrow p + n + {}^4\text{He}$, and the fact that two peaks are observed is a kinematic effect. This can be seen as follows. The measurements of Fukunaga *et al.*¹¹ on the reaction $\alpha(d, p){}^5\text{He(g.s.)}$, at the bombarding energy $E_d = 14.2$ MeV, show a large probability for proton emission in the forward direction, that is, in the direction of the incident deuteron. Since the center-of-mass energies for that experiment and the present one are comparable (9.4 and 12.9 MeV, respectively) this fact should be of relevance to the present experiment. Hence we take as a simple model for the reaction the one represented by the velocity diagram of Fig. 6. Here the velocity vectors involved are the velocity V_c of the center of mass of the $\alpha + d$ system, the velocity V_s of the ${}^5\text{He(g.s.)}$ system relative to the center of mass of the $\alpha + d$ system (corresponding to proton emission in the direction opposite to that of the incident α particle), the velocity $V_n^{(c)}$ of the neutron from the breakup of ${}^5\text{He}$ ($Q = +0.96$ MeV) with respect to the center of mass of ${}^5\text{He}$, and the laboratory velocity $V_n^{(L)}$ of the neutron corresponding to the laboratory scattering angle θ_L . It can be seen from the figure that $V_n^{(L)}$ is double valued for $\theta_L \leq 19^\circ$, in qualitative agreement with the neutron spectra in Fig. 4. Furthermore, the corresponding neutron laboratory energies calculated from the two values of $V_n^{(L)}$ at each angle θ_L are in good agreement with the peak positions observed in the 15 and 18° neutron energy spectra. It is interesting to note that such a double peak should have been observable in the experiment by Rybakov,

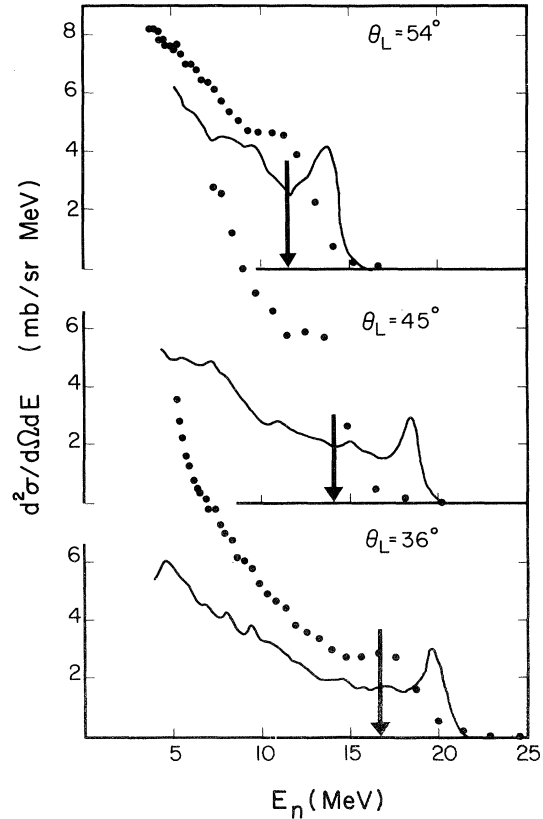


FIG. 5. Laboratory differential cross sections for neutron and proton emission at various laboratory angles, from $\alpha + d$. The abscissa represents laboratory neutron or proton energy. The circles represent neutron data obtained with a deuterated polyethylene target. The solid curves represent proton data taken from Ref. 10, measured at 41.6-MeV α -particle bombarding energy. The arrows indicate the expected neutron energy for the process $\alpha + d \rightarrow n + {}^5\text{Li(g.s.)}$.

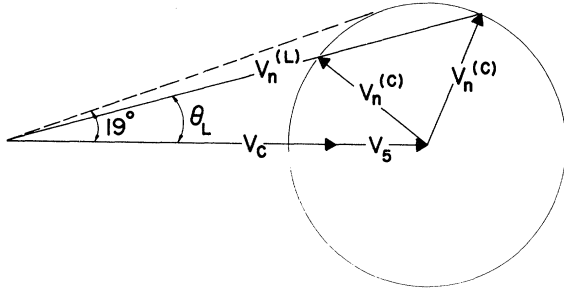


FIG. 6. Velocity diagram for the process $\alpha + d \rightarrow p + n + {}^4\text{He}$ at 38.8-MeV α -particle bombarding energy. The vectors are identified in the text of Sec. IV.

Sidorov, and Vlasov,⁶ in which the neutron energy spectrum from the 34.6-MeV α bombardment of deuterium was observed at 0° . Upon transforming their result to laboratory coordinates, the resulting spectrum is very similar in shape to the 15° spectrum of Fig. 4, but contains only one peak due to the fact that the low-energy portion of the spectrum was not recorded. It is also appropriate to add that if a velocity diagram similar to Fig. 6 is constructed for the analogous sequential reaction, $\alpha + d \rightarrow n + {}^5\text{Li}(\text{g.s.}) \rightarrow n + p + {}^4\text{He}$, a double peak is predicted in the proton energy spectra at laboratory angles smaller than 28° . The predicted position of the higher-energy peak does in fact agree with the positions of the absolute maxima in the

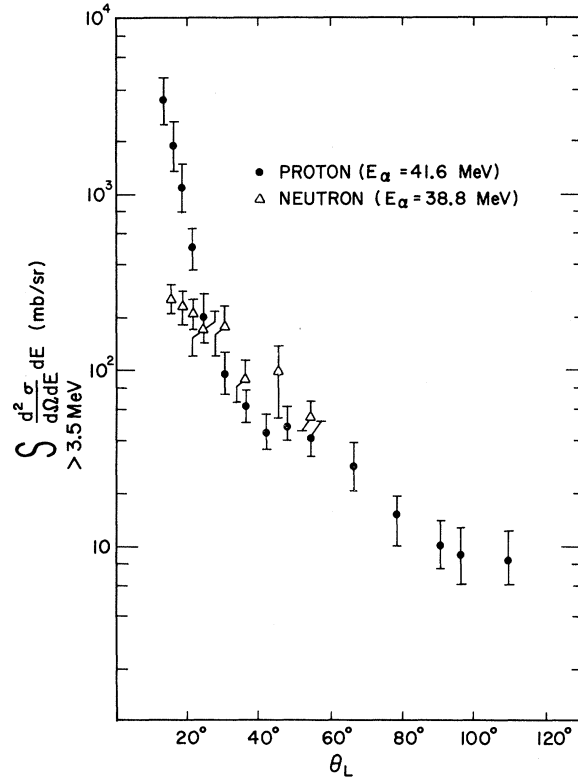


FIG. 7. Energy-integrated laboratory angular distributions for neutron (triangles) and proton (circles) emission from $\alpha + d$. The neutron points are based on the data of Figs. 4 and 5. The proton points are from Ref. 10.

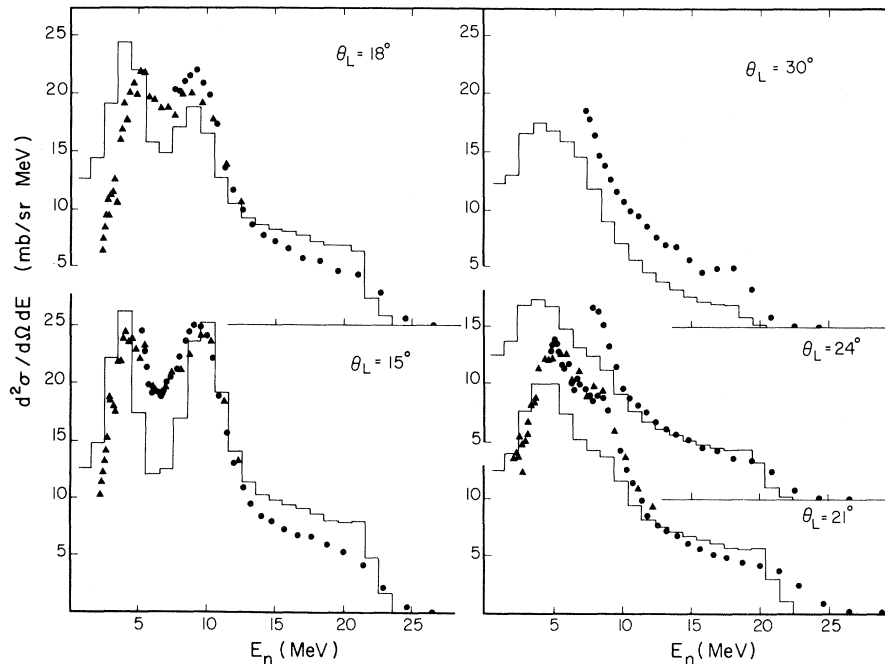


FIG. 8. Comparison of measured neutron energy spectra from $\alpha + d$ for $E_\alpha = 38.8$ MeV (plotted points) with the new impulse approximation calculations of Nakamura for $E_\alpha = 38.2$ MeV (histograms).

proton energy spectra of Fig. 4. In all cases the predicted position of the lower-energy peak lies below the experimental cutoff energy.

A third feature of the data of Figs. 4 and 5 is the remarkable difference between the magnitudes of the neutron and proton cross sections at small angles. This feature is also brought out in Fig. 7 in which the neutron and proton cross sections at each angle, integrated over all neutron or proton energies larger than 3.5 MeV are plotted versus the angle. (Those neutron spectra which do not include data as low as 3.5 MeV were arbitrarily extended for this purpose, where the extension was guided by considerations based on the Nakamura theory discussed below. A conservative error equal to half the amount added to the cross section was used in these cases.) From Fig. 7 one can calculate the contribution to the total reaction cross section for $\alpha + d \rightarrow n + p + \alpha$ from the angular ranges in which data exist. For proton emission one obtains 660 ± 230 mb for the angular range 13 to 109° ; for neutron emission, 280 ± 80 mb for the angular

range 15 to 54° . Over the full 180° angular range and including all energies of emission the two total reaction cross sections must of course be equal at the same bombarding energy.

Shanley¹⁸ has calculated the total reaction cross for *deuteron* bombarding energies up to 30 MeV, using a Faddeev approach, and the results agree quite well with three experimental measurements in the vicinity of 10-MeV deuteron energy. At 20-MeV deuteron energy (corresponding to 40-MeV α -bombarding energy) Shanley's calculations predict 420 mb. The rapid increase in the experimental proton emission cross section at small angles suggests, however, that there will be a substantial contribution to the total cross section from angles smaller than 13° . For example, even in the extreme case of a proton cross section which does not increase below 13° but instead remains at the 13° value the additional contribution will be 530 ± 190 mb, increasing the estimated (α, p) total cross section to 1190 ± 300 mb. In contrast, if the neutron data of Fig. 7 are extrapolated to the full 180° angular range by assuming a simple decreasing exponential dependence on angle, then one obtains a total reaction cross section of 540 ± 150 mb, in fair agreement with Shanley's calculated value. It might be noted here that the measurements of Rybakov give a value of 300 ± 40 mb for the 0° laboratory differential cross section for neutron emission induced by 34.6-MeV α particles, quite consistent with the trend of the present data. Thus the absolute magnitude of the experimental proton cross sections of Nagatani *et al.* appears to be inconsistent with other related experimental and theoretical work.

Finally, the present data can be compared with calculations¹⁹ based on a new impulse approximation theory due to Nakamura.²⁰ The comparison is shown in Figs. 8 and 9. For angles less than or equal to 30° , the agreement with the experimental data in both shape and magnitude is quite good. It should be noted that the theory contains no free parameters, and has not been normalized to fit the data. A common failure of previous impulse approximation theories is their overestimation of the cross section. Nakamura's theory does not show such a defect in the comparison with our results.

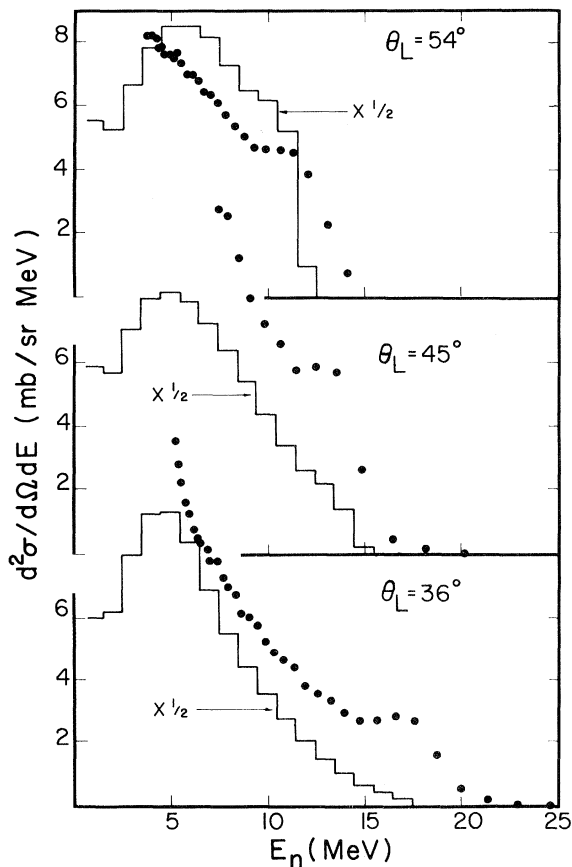


FIG. 9. Comparison of measured neutron energy spectra from $\alpha + d$ for $E_\alpha = 38.8$ MeV (plotted points) with the new impulse approximation calculations of Nakamura for $E_\alpha = 38.2$ MeV (histograms).

ACKNOWLEDGMENTS

We wish to acknowledge useful discussions with J. V. Noble and J. W. Watson, as well as the invaluable assistance of E. P. Chamberlin and F. N. Rad in obtaining and processing the data.

*Work supported by the U. S. Atomic Energy Commission under Contract No. AT-(40-1)-3398.

†Present address: Institut für Experimentelle Kernphysik der Universität (TH) Karlsruhe auf dem Kernforschungszentrum Karlsruhe, 75 Karlsruhe, Postfach 3640, Germany.

¹J. C. Allred, D. K. Froman, A. M. Hudson, and L. Rosen, *Phys. Rev.* **82**, 786 (1951).

²R. L. Henkel, J. E. Perry, Jr., and R. K. Smith, *Phys. Rev.* **99**, 1050 (1955).

³G. F. Bogdanov, N. A. Vlasov, S. P. Kalinin, B. V. Rybakov, and V. A. Sidorov, *Zh. Eksperim. i Teor. Fiz.* **30**, 981 (1956) [transl.: *Soviet Phys. - JETP* **3**, 793 (1956)].

⁴E. W. Warburton and J. N. McGruer, *Phys. Rev.* **105**, 639 (1957).

⁵K. P. Artemov and N. A. Vlasov, *Zh. Eksperim. i Teor. Fiz.* **39**, 1612 (1960) [transl.: *Soviet Phys. - JETP* **12**, 1124 (1961)].

⁶B. V. Rybakov, V. A. Sidorov, and N. A. Vlasov, *Nucl. Phys.* **23**, 491 (1961).

⁷H. W. Lefevre, R. R. Borchers, and C. H. Poppe, *Phys. Rev.* **128**, 1328 (1962).

⁸H. J. Erramuspe and R. J. Slobodrian, *Nucl. Phys.* **49**, 65 (1963).

⁹G. G. Ohlsen and P. G. Young, *Phys. Rev.* **136**, B1632 (1964).

¹⁰K. Nagatani, T. A. Tombrello, and D. A. Bromley, *Phys. Rev.* **140**, B824 (1965).

¹¹K. Fukunaga, H. Nakamura, T. Tanabe, K. Hosono, and S. Matsuki, *J. Phys. Soc. Japan* **22**, 28 (1967).

¹²R. E. Warner and R. W. Bercaw, *Nucl. Phys.* **A109**, 205 (1967).

¹³T. Tanabe, *J. Phys. Soc. Japan* **25**, 21 (1968).

¹⁴L. C. Northcliffe, C. W. Lewis, and D. P. Saylor, *Nucl. Instr. Methods* **69**, 789 (1970).

¹⁵H. G. Blosser and R. St. Onge, *Bull. Am. Phys. Soc.* **14**, 533 (1969).

¹⁶J. R. Stehn, M. D. Goldberg, B. A. Magurno, and R. Wiener-Chasman, Brookhaven National Laboratory Report No. BNL-325 (unpublished).

¹⁷C. W. Lewis and J. M. Blair, *Nucl. Instr. Methods* **35**, 261 (1965).

¹⁸P. E. Shanley, *Phys. Rev.* **187**, 1328 (1969).

¹⁹H. Nakamura, private communication.

²⁰H. Nakamura, *Nucl. Phys.* **A137**, 51 (1969).

Off-Shell t Matrix for the Boundary-Condition Model*

D. D. Brayshaw

Columbia University, New York, New York 10027

(Received 31 August 1970)

An off-shell t matrix is developed for the boundary-condition model in the general case of coupled partial waves. This development is facilitated by the use of a method for solving the Lippmann-Schwinger equation directly for potentials of the square-well type. The t matrix obtained is shown to be unique under some rather mild assumptions as to analyticity and asymptotic behavior. An integral equation of the Lippmann-Schwinger type is obtained for the t matrix in the more realistic problem of boundary condition plus external potential.

INTRODUCTION

Perhaps the chief difficulty in constructing potential models to represent the effective nucleon-nucleon (N - N) interaction is the question of what to do about extremely short-range effects. In the region of small internucleon separation, it has long been recognized¹ that a local potential cannot adequately describe multimeson exchange and other inherently nonlocal higher-order effects suggested by the meson theory of nuclear forces. Consequently, attempts have been made to simulate the infinite complexity of the interaction in this region by introducing either highly repulsive short-range potentials (soft cores),² or simple nonlocal devices such as the hard core³ and its generalization, the boundary-condition model (BCM).⁴

Together with appropriate longer-range components, all of these approaches can be employed to

yield models⁵ which give theoretical predictions in quite good agreement with the N - N scattering data up to the vicinity of 350 MeV. However, because of continuing improvements in computer facilities and computational techniques, it should be possible in the near future to discriminate between these models by employing them in the Faddeev equations⁶ to calculate properties of the three-nucleon system. In doing so, one must learn how to properly incorporate singular two-body interactions such as the hard-core and BCM into the three-body framework. One of the virtues of the Faddeev formulation from this standpoint is that the dependence on the two-nucleon potentials can be entirely eliminated in favor of the off-shell two-nucleon t matrices.⁷ On the other hand, it is not entirely clear what one should regard as the appropriate off-shell t matrix in such cases. It cannot, for example, be defined as the solution of the Lipp-